

Influence of magnetic field on the transition temperature of the $(\text{Cr}_{84}\text{Re}_{16})_{89.6}\text{V}_{10.4}$ alloy

BS Jacobs, CJ Sheppard and ARE Prinsloo

Department of Physics, University of Johannesburg, PO Box 524, Auckland Park, 2006

E-mail address: sjacobs@uj.ac.za

Abstract. In this study, the variation of the Néel transition temperature of the $(\text{Cr}_{84}\text{Re}_{16})_{89.6}\text{V}_{10.4}$ alloy is investigated through the application of magnetic field. Magnetic susceptibility (χ) was measured as a function of temperature (T) in the temperature range $2 \text{ K} \leq T \leq 200 \text{ K}$. The sample was cooled to 2 K in zero field, followed by measurements being collected upon warming the sample in static applied fields (H) in the range $0.01 \text{ T} \leq H \leq 6.5 \text{ T}$. The $\chi(T)$ curves obtained for the various applied fields show a clear peak and the temperature associated with the peak was taken as the Néel temperature, T_N . Results indicate that the sharpness of the peak improves on increasing H , with an accompanying suppression of T_N . The $T_N(H)$ curve varies exponentially with applied field up to 6.5 T, the highest applied field used in the present study. This is linked to previously reported quantum critical behaviour in Cr.

1. Introduction

Long range spin-density-wave (SDW) antiferromagnet ordering occurs in chromium below 311 K, its Néel temperature (T_N) [1]. The characteristic changes in the transport properties observed in the vicinity of T_N can be attributed to gap formation in portions of the Fermi surface as itinerant electron antiferromagnetism is established in this material [1].

Studies on the possible tuning of pure Cr and certain of its alloys through a quantum critical point (QCP) have intensified in recent years, as is reflected in literature [2, 3, 4]. This resulted from reports that indicated that charge density wave (CDW) and SDW systems appear to be good candidates for investigations into quantum critical behaviour (QCB), in which quantum fluctuations cause a disruption in electron pairing and results in the restoration of the metallic Fermi surface (FS) [5, 6, 7]. In CDW and SDW systems the interaction strengths are considered relatively weak, therefore allowing relatively easy experimental access to the quantum critical point in comparison to strongly correlated systems [7].

A quantum critical point (QCP) occurs when the phase transition temperature is driven to zero by the application of a tuning parameter such as magnetic field, pressure or by doping [2]. No thermal fluctuations exist at absolute zero; instead, quantum fluctuations drive the transitions in accordance with Heisenberg's uncertainty principle [8]. A state of constant agitation is adopted at the QCP, even when thermal motion ceases, in order to abide by the uncertainty principle [9].

The three main experimental methods used to tune a system towards a putative quantum critical point are doping, pressure and magnetic field application. Doping a particular alloy in order to drive it to a QCP is regularly used by experimentalists, however fine doping of the alloy close to the QCP is

difficult and it also induces disorder in the system [10]. Another control parameter used is applied pressure. Although fine tuning of this control parameter is possible close to the QCP, there are other associated difficulties that are introduced by the pressure cell itself [10]. Hence, magnetic field has recently been used more frequently to probe and understand critical behaviour [10, 11].

According to Fischer *et al.* [10], magnetic field will have two main effects. Firstly, it suppresses or induces magnetic order and secondly, it causes a precession of the magnetic moments perpendicular to the magnetic field and therefore modifies the dynamics of the order parameter. In this paper [10] the authors also argue that the susceptibility, $\chi = \partial M / \partial B$, is the thermodynamic quantity that will show the most substantial change upon approaching the QCP.

With the discovery of QCB in Cr and its alloys, not much work has been reported on investigations into QCB induced by the application of magnetic field in these alloys. However, extensive work on pressure induced QCB in Cr has been reported by Jaramillo *et al.* [12, 13]. It was found that the order parameter varied exponentially with the tuning parameter at low pressures of less than 7 GPa. This is referred to as the Bardeen-Cooper-Schrieffer (BCS) regime and in this pressure range, Cr is modelled by a BCS-like weak coupling theory. However, at pressures above 7 GPa and low temperatures, this exponentially tuned ground state is destabilized and at 10 GPa the SDW is terminated by a quantum phase transition [12].

Signatures of QCB have previously been reported [2, 3, 4] in electrical resistivity (ρ), magnetic susceptibility (χ), Hall coefficient (R_H) and Sommerfeld coefficient of specific heat (γ) measurements of Cr and its alloys. Even though the QCP occurs at absolute zero, its influence and the corresponding signatures occur at low, finite temperatures in the quantum critical regime. Considering these results, possible quantum critical behaviour in the $(\text{Cr}_{84}\text{Re}_{16})_{100-y}\text{V}_y$ alloy system has been previously investigated utilizing ρ , χ , R_H and γ [14]. A putative QCP was reported at a critical concentration of $y_c \approx 10.5$ in this alloy system. The $\chi(T)$ results on the $(\text{Cr}_{84}\text{Re}_{16})_{100-y}\text{V}_y$ alloy system showed weak anomalies at the phase transition temperatures that becomes more pronounced with increase in the V concentration. This corresponds to observations by Yeh *et al.* [3] that investigated the QCB in the $\text{Cr}_{1-x}\text{V}_x$ alloy system through χ measurements. This system shows antiferromagnetic ordering below the critical concentration (x_c) of 0.035. In their results, a reduction in χ is observed on entering the ordered state for $x < x_c$ as is expected for Cr and its alloys [1]. This is explained in terms of the band theory and the reduction of the density of states at the Fermi level on SDW formation [3].

Extending the quantum criticality studies on the $(\text{Cr}_{84}\text{Re}_{16})_{100-y}\text{V}_y$ alloy system, the present study reports the results of the effect of magnetic field on the magnetic susceptibility of the $(\text{Cr}_{84}\text{Re}_{16})_{89.6}\text{V}_{10.4}$ antiferromagnetic alloy by studying $\chi(T)$ at different constant applied magnetic fields. The selected alloy has V concentration very close to the previously reported critical concentration of the $(\text{Cr}_{84}\text{Re}_{16})_{100-y}\text{V}_y$ system [14] and the vision is to explore possible QCB in this sample by considering a new tuning parameter, namely magnetic field.

2. Experimental

The polycrystalline $(\text{Cr}_{84}\text{Re}_{16})_{89.6}\text{V}_{10.4}$ alloy was prepared from the constituent metals Cr, Re and V of mass fractional purities 99.99%, 99.99% and 99.8%, respectively, by repeated arc melting in purified argon atmosphere. The sample was sealed in a quartz ampoule filled with pure argon gas at low pressure and annealed at 1343 K for seven days followed by quenching in iced water. Powder X-ray diffraction (XRD) analyses confirmed the expected body centred cubic (bcc) crystal structure. Electron microprobe analyses were used to determine the homogeneity and elemental compositions of Cr, Re and V in the sample. A portion of the sample in the form of a disc was prepared from the alloy ingot using spark erosion technique. Magnetic susceptibility (χ) as a function of temperature (T) was measured, on this disc, in the temperature range $1.9 \text{ K} \leq T \leq 200 \text{ K}$ using the Quantum Design Magnetic Property Measurement System (MPMS). The sample was cooled to 1.9 K in the absence of a field, followed by the measurements being collected upon warming the sample in static applied fields (H) in the range 0.01 T to 6.5 T.

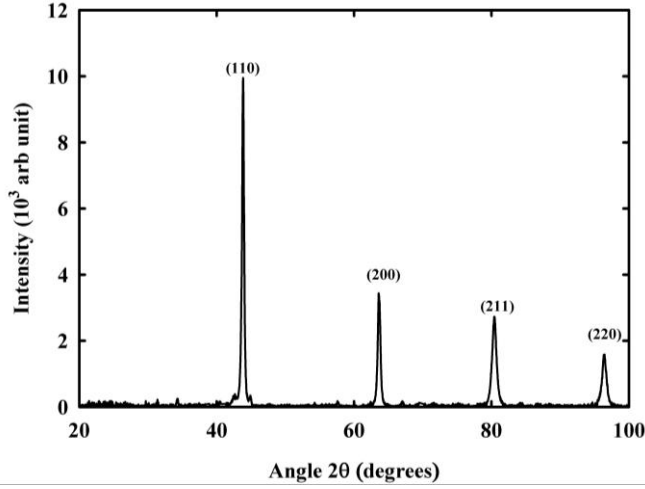


Figure 1: The XRD pattern for the $(\text{Cr}_{84}\text{Re}_{16})_{89.6}\text{V}_{10.4}$ sample with (hkl) Miller indices of the various reflections expected for the profile of bcc Cr indicated.

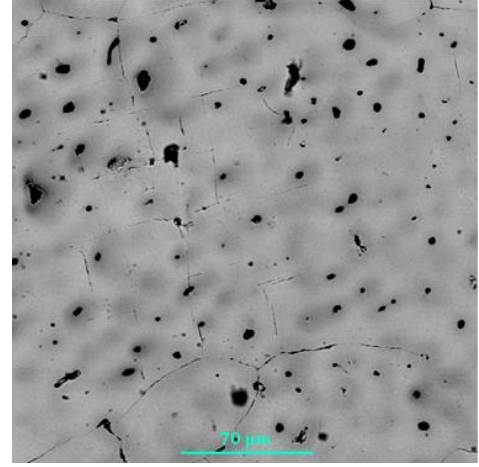


Figure 2: The backscattered-electron image obtained on the $(\text{Cr}_{84}\text{Re}_{16})_{89.6}\text{V}_{10.4}$ sample.

	at.% Cr	at.% Re	at.% V
Actual Average Elemental Compositions	85.0 ± 1.3	15.0 ± 1.2	10.4 ± 0.2
Dark regions in back scattered image	85.0 ± 0.8	15.0 ± 0.7	9.6 ± 0.2
Light regions in back scattered image	81.9 ± 0.5	18.1 ± 0.3	10.2 ± 0.2

Table 1: Elemental concentrations obtained from electron microprobe analyses on the $(\text{Cr}_{84}\text{Re}_{16})_{89.6}\text{V}_{10.4}$ sample. The dark and the light regions refer to backscattered-electron image shown figure 2.

3. Results and discussion

Figure 1 shows the XRD pattern for the $(\text{Cr}_{84}\text{Re}_{16})_{89.6}\text{V}_{10.4}$ sample. The entire profile in the $(\text{Cr}_{84}\text{Re}_{16})_{89.6}\text{V}_{10.4}$ spectrum is well fitted to the XRD pattern of pure bcc Cr by adjusting the lattice parameter of pure Cr (0.28839 nm) to 0.2926 nm for this alloy. No additional peaks are detected to within instrumental resolution indicating that the alloy formed in the bcc phase of pure Cr.

Electron microprobe analyses of the samples showed good homogeneity of the alloy and the average actual elemental compositions of Cr, Re and V are listed in Table 1. Figure 2 shows the backscattered-electron image obtained on this sample. The light and the dark regions observed in the image differ slightly in concentration as is summarized in Table 1. Also clear in this image are black spots. The spots were also analysed and found to be either empty pores or in certain cases the wavelength dispersive X-ray spectra analyses showed the presence of oxygen within these dark inclusions. Further analyses showed that these were inclusions of predominantly Cr_2O_3 and V_2O_3 . These inclusions cover approximately 2% of the image having a surface area of about $61500 \mu\text{m}^2$. Considering that $\chi(T)$ measured at 0.01 T, $\rho(T)$ and $S(T)$ measurements all give similar T_N -values [14], it is however not expected that, at this low concentration levels, these inclusions will have a substantial influence on the Néel temperatures determined from $\chi(T)$ and that effects of these inclusions may be neglected in the present study.

The $\chi(T)$ data for a series of $(\text{Cr}_{84}\text{Re}_{16})_{100-y}\text{V}_y$ alloys were previously reported [14]. Weak anomalies are seen in the $\chi(T)$ curves at the phase transition temperatures, becoming more pronounced as the V concentration is increased [14]. For samples with $y < 10.4$, χ decreases almost linearly on cooling for $T > T_N$, followed by an anomalous sharper downturn in χ on cooling through T_N , similar to the $\chi(T)$ -behaviour usually observed in Cr and certain of its alloys in the vicinity of T_N [1]. The anomalous downturn in the $\chi(T)$ curves below T_N is ascribed to a decrease in the density of

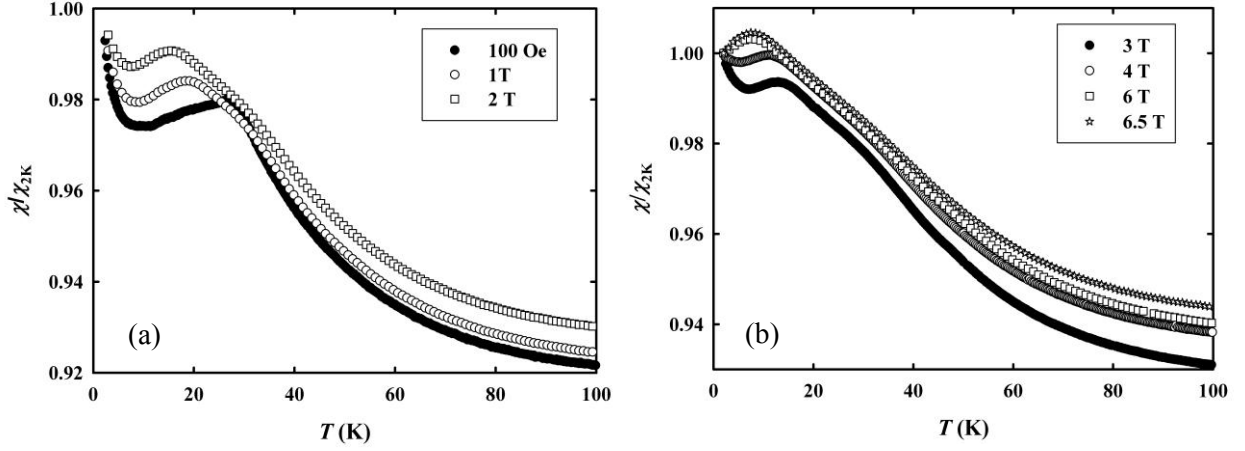


Figure 3 (a) and (b): Temperature dependence of χ/χ_{2K} at various static fields. The experimental error associated with absolute values of χ is approximately 0.1% and originates from the measurements of the masses of the samples.

electron states at the Fermi energy, $N(E_F)$, when the nested parts of the electron and hole Fermi sheets these alloys are annihilated on SDW formation below [1]. On cooling the $(\text{Cr}_{84}\text{Re}_{16})_{89.6}\text{V}_{10.4}$ alloy from the paramagnetic phase down through T_N , nesting of the electron and hole FS sheets should also result in a reduction in the density of states due to the appearance of the SDW energy gap, thus explaining the reduction in $\chi(T)$ observed for this alloy for $T < T_N$. However, a different behaviour is observed in the region $T > T_N$. For this sample, the linear decrease in $\chi(T)$ on cooling from $T > T_N$ is not seen. Instead, a clear increase is observed in this temperature range on cooling, ending in a maximum value for χ at T_N , followed by the expected decrease on further cooling, resulting in a clear peak at T_N . This might be indicative of the presence local magnetic moments in the paramagnetic phase. A similar behaviour was observed by Sousa *et al.* [15] in the $\text{Cr}_{100-x}\text{Al}_x$ alloy system for the commensurate (C) SDW alloys with $x = 2.23$ and 2.83 . De Oliveira *et al.* [16] also observed similar peaks at T_N in the $\text{Cr}_{100-y}\text{V}_y$ alloy system for incommensurate (I) SDW alloys with $y \leq 0.67$. They attributed the peaks in χ at T_N to a local SDW that is formed around the V atoms, resulting in Curie-Weiss paramagnetism above T_N [16]. This might then also be of importance to consider in the present $(\text{Cr}_{84}\text{Re}_{16})_{89.6}\text{V}_{10.4}$ alloy.

Against this background, we can now consider the temperature dependence of χ/χ_{2K} in various applied static fields (H) for the $(\text{Cr}_{84}\text{Re}_{16})_{89.6}\text{V}_{10.4}$ alloy. These results are shown in figure 3(a) and (b). Each curve shows a well-defined anomaly in the form of a clear peak and for this alloy, the temperature associated with the peak was taken as T_N . The T_N value obtained in this way for the 0.01 T field corresponds well with T_N values obtained for the same sample through $\rho(T)$ (considering $d\rho(T)/dT$) and $S(T)$ measurements reported in a previous study [14]. It is also important to note that the T_N -anomaly observed in the $\chi(T)$ measurements at 0.01 T for this sample is better defined than those observed in the $\rho(T)$ and $S(T)$ curves [14], emphasizing the fact that susceptibility measurement is a sensitive tool for probing the magnetic transition in this specific alloy. The slight low temperature upturn observed in the curves shown in figure 3 for measurements with $H \leq 4$ T may be attributed to a Curie tail arising from oxide impurities, that were identified in the backscattered-electron image shown in figure 2. Considering the results shown in figure 3 (a) and (b), it is evident that the sharpness of peak observed at T_N improves with field. Furthermore, the application of field suppresses T_N .

The field dependence of T_N obtained from the curves in figure 3 (a) and (b) is shown in figure 4. T_N varies exponentially with applied field, as is indicated by the exponential fit to the data (see the broken line in figure 4). The broken line indicates the fit of an equation of the form $y = Ae^{(-x/t)} + y_0$ to the data, with $A = (20.1 \pm 1.2)$ K, $t = (2.8 \pm 0.4)$ T and $y_0 = (5.8 \pm 1.2)$ K

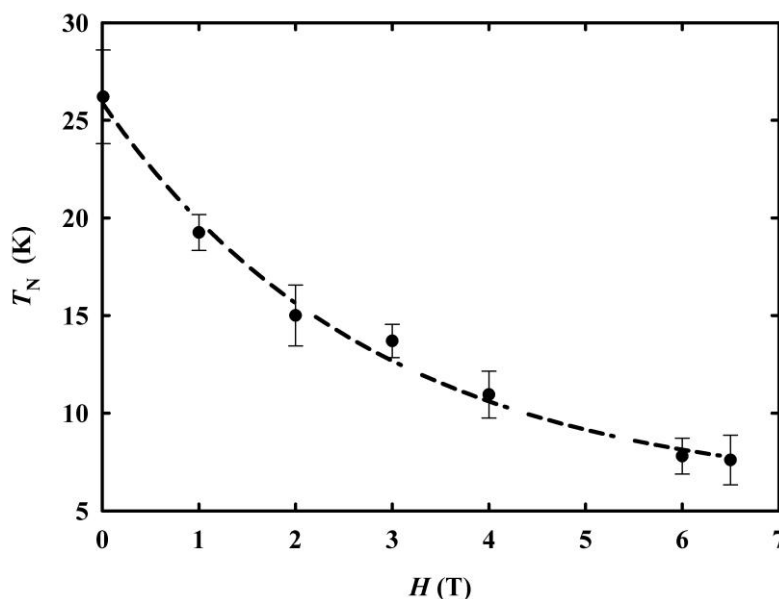


Figure 4: The field dependence of T_N obtained from the $\chi(T)$ curves shown in figure 3. The broken line indicates the fit of an equation of the form $y = Ae^{(-x/t)} + y_0$ to the data.

The exponentially decaying behaviour in the ordering parameter with respect to the tuning parameter is reminiscent of the work by Jaramilo *et al.* [12, 13] on a pressure induced quantum criticality in pure Cr. In their work the order parameter, T_N , investigated varied exponentially at low pressures of less than 7 GPa. However, at high pressures and low temperatures this exponentially tuned ground state is destabilized and the spin density wave (SDW) is terminated by a quantum phase transition [12]. It is therefore hypothesized that the $(\text{Cr}_{84}\text{Re}_{16})_{89.6}\text{V}_{10.4}$ alloy presently investigated is still in the BCS-regime up to the maximum applied field we could attain and that at higher magnetic fields and low temperatures this exponentially tuned ground state can be destabilized and the SDW might be terminated by a quantum phase transition.

4. Conclusion

The results presented here on the antiferromagnetic $(\text{Cr}_{84}\text{Re}_{16})_{89.6}\text{V}_{10.4}$ alloy provide an overview on this sample's behaviour in the presence of magnetic field. Measurements need to be extended to include $\chi(T)$ measurements in higher applied fields. This might result, at high applied magnetic fields and low temperatures, in the destabilization of this exponentially tuned ground state and the termination of the SDW by a quantum phase transition.

Acknowledgments

Financial support from the South African NRF (Grant numbers 80631, 80928 and 80626) is acknowledged.

References

- [1] Fawcett E, Alberts H L, Galkin V Y, Noakes D R and Yakhmi J V 1994 *Rev. Mod. Phys.* **66** 25
- [2] Lee M, Hussman A, Rosenbaum T F and Aeppli G 2004 *Phys. Rev. Lett* **92** 187201
- [3] Yeh A, Soh Y A, J Brooke J, Aeppli G, Rosenbaum T F and Hayden S M 2002 *Nature* **419** 459
- [4] Takeuchi J, Sasakura H and Masuda Y 1980 *J. Phys. Soc. Japan* **49** 508
- [5] Altshuler B L, Ioffe L B and Millis A J 1995 *Phys. Rev. B* **52** 5563

- [6] Metlitski MA and Sachdev S 2010 *Phys. Rev. B* **82** 075128
- [7] Feng Y, Wang J, Jaramillo R, van Wezeld J, Haravifarda S, Srajer G, Liue Y, Xuf Z-A, Littlewoodg PB and Rosenbaumb 2012 *PNAS*. **109**(19) 7229
- [8] Sachdev S and Keimer B 2011 *Physics Today* 29
- [9] Coleman P and Schofield AJ 2005 *Nature* **433**226
- [10] Fischer I and Rosch A 2005 *Phys. Rev. B* **71** 184429
- [11] Carretta P, Giovannini M, Graf MJ, Papinutto N, Rigamonti A and Sullivan K 2006 *Physica B* **378-380** 84-86
- [12] Jaramillo R, Feng Y and Rosenbaum TF 2010 *J. Appl. Phys.* **107** 09E116
- [13] Jaramillo R, Feng Y, Wang J and Rosenbaum TF 2010 *PNAS*. **107** 13631
- [14] Jacobs BS, Prinsloo ARE, Sheppard CJ and Strydom AM 2013 *J. Appl. Phys* **113** 17E126
- [15] Sousa J B, Amado M M, Pinto R P, Pinheiro M F, Braga M E, Moreira J M, Hedman L E, Åström H U, Khlaif L, Walker P, Garton G and Hukin D 1980 *J. Phys. F: Metal Phys.* 10 2535
- [16] De Oliveira A J A, Ortiz W A, de Lima, O F and de Camargo P C 1997 *J. Appl. Phys.* 81 4209